Available online at www.sciencedirect.com

SCIENCE DIRECT

Cement and Concrete Research 35 (2005) 1332–1343

Cement and Concrete Research

Effect of magnesium and sulfate ions on durability of silica fume blended mixes exposed to the seawater tidal zone

Eshmaiel Ganjian[a,*], Homayoon Sadeghi Pouya[b]

[a]School of Science and Environment, University of Coventry, Sir John Laing Building, Priory St., Coventry CV1 5FB, UK
[b]Department of Civil and Structural Engineering, University of Sheffield, Sir Fredrick Mappin Building, Mappin St., Sheffield S1 3JD, UK

Received 25 May 2004; accepted 17 September 2004

Abstract

The effect of silica fume on deterioration resistance to sulfate attack in seawater within tidal zone and simulated wetting–drying condition has been studied in Portland cement concretes and pastes containing silica fume (SF) with/without ground granulated blast furnace slag (GGBS). Changes in the compressive strength and capillary water absorption of specimens as a function of SF content have been investigated combined with phases determination by means of scanning electron microscopy and X-ray energy dispersion analysis. The strength change factors (SCFs) of specimens with SF (the more SF content, the higher strength loss) were greater than that of the mixes without SF or cured under tap water. Mg^{2+} ion originated attack found to be the dominating deterioration mechanism as confirmed by X-ray and chemical analyses.

Further, the incorporation of GGBS with SF mixes in different exposure conditions led to the worst performance in all of the test environments. Lower cement content and hydration rate accompanied with particular chemical composition of GGBS made concrete and paste specimens to be more susceptible to deleterious seawater environment.

Keywords: Concrete; Durability; Silica fume; Granulated blast furnace slag; X-ray diffraction

1. Introduction

Silica fume has been used as high pozzolanic reactive cementitious material to make high-performance concrete in the severe conditions [1,2]. This mineral admixture has highly been used in severe environmental conditions despite its several mixing and curing problems, because of its acceptable early age strength development [3,4,5]. The hydration mechanism and properties of secondary C–S–H made by pozzolanic reaction have been studied by many investigators [4]. However, pozzolanic C–S–H formed by silica fume–calcium hydroxide reaction might be different in respect of the amount of molecular water, C/S ratio and density [6]. Moreover, because of its rather different characteristics, pozzolanic gel has high potential to contribute in reactions with other internal or external ions such as Al, Cl and alkalines [7,8].

Deterioration and durability of concrete structures which are exposed to harmful ions or chemicals are subject of the major discussions for service life of high cost or key concrete structures. Sulfate attack has been reported to be a cause of damage to concrete for over a century. Many of the reinforced and unreinforced structures exposed to seawater will suffer from deleterious chemical reactions between hardened cement compositions and different sulfate ions in cementitious matrix of the structures.At least six types of reactions could be described by sulfate attack. The most common reactions often used to explain the defined sulfate attack are ettringite and gypsum formation [9]. It is generally accepted that sodium and magnesium sulfate attacks of hydrated cement matrix take place due to the reaction of

* Corresponding author. Tel.: +44 24 7688 7625; fax: +44 24 7688 8296.
E-mail address: E.Ganjian@Coventry.ac.uk (E. Ganjian).

0008-8846/$ - see front matter © 2004 Elsevier Ltd. All rights reserved.
doi:10.1016/j.cemconres.2004.09.028

Table 1
Chemical analysis for cement, silica fume (SF) and ground granulated blast furnace slag (GGBS)

	Cement	SF	GGBS
Chemical composition (%)			
SiO_2	21.7	91.7	33.03
Al_2O_3	4.9	1.27	10.87
Fe_2O_3	3.2	1.45	0.25
CaO	62.4	1.69	38.45
MgO	3.58	0.6	10.26
SO_3	1.84	0.45	<0.1
Na_2O	0.35	–	0.65
K_2O	0.95	–	0.78
Cl	0.017	0.08	0.007
Loss on ignition	1	2	0.25
Mineralogical components (%)			
C_3S	46.3	–	–
C_2S	27.12	–	–
C_3A	7.58	–	–
C_4AF	9.73	–	–

sulfate ions with calcium hydroxide and calcium aluminate phases, forming gypsum and ettringite. Furthermore, in the case of magnesium sulfate attack, brucite ($Mg(OH)_2$), which has low solubility, is produced and is assumed to envelop the remainder of the cement gel and protect it against further deterioration [6,10,11]. However, Turker [12] reported that this process is effective at early stages. At later stages, on the other hand, deterioration processes due to brucite will become dominant.

Another reaction which can take place by magnesium sulfate is the degradation and disintegration of C–S–H gel to M–S–H gel, which is non-cementitious product and leads to softening of the cement matrix. [10,13,14]. From the forgoing, it can be concluded that the amount of calcium hydroxide should be limited to a minimum, to make concrete durable and also prevent the C–S–H gel from softening and being in tacked by ingress ions. The concrete mixtures containing silica fume are superior owing to the fact that the pore structures are finer and the amount of calcium hydroxide is less than the ordinary mixes [15].

In addition to chemical deterioration, the mechanism sometimes called 'salt crystallization', which usually involves repeated dissolution of the solid salts and recrystalization, will occur in concrete pores. Slight variation in temperature and relative humidity causes the reversible reactions to form $Na_2SO_4 \cdot 10H_2O$, $MgSO_4 \cdot H_2O$ O and $MgSO_4 \cdot 6H_2O$. This is accompanied with large expansion which indeed is not salt crystallization. These large expansions cause tension stress far greater than the concrete bearing capacity and therefore lead to rupture of cementitious matrix [9]. The enhanced pore structure of silica fume concretes can contribute in the improvement of concrete durability against the above phenomena [16].

In this paper, strength change factor (SCF) and pore structure factor (PSF) of concrete and paste specimens exposed to two different long-term deleterious environments are compared. The test results are then discussed with the particular attention to chemical, XRD and X-ray energy dispersion analyses.

2. Experimental procedure

An experimental program was designed to produce a high-performance concrete and paste for the best protection in marine tidal zone by using optimum silica fume [17] and ground granulated blast furnace slag (GGBS) percentage mass replacement for the type II cement. The materials used and the experimental procedures are described in the following sections.

2.1. Materials used and specimens preparation

In this research (ASTM) C 150 type II cement was used. Silica fume (SF), obtained from Iran Ferro Alloy Industry, and GGBS produced by Isfahan iron factory were used for partial replacement of cement in the concretes and pastes. The mixes incorporating 7% and 10% SF as a cement replacement were blended with and without 50% GGBS by weight of cement. Complex oxides of cement were calculated using Bogue's equations. Complex oxides together with chemical components of silica fume and GGBS are given in Table 1. The specific gravity of the cement used was 3.15 and its specific surface was 290.8 m^2/kg (Blaine). The nitrogen Brunauer–Emmett–Teller (BET) fineness of the SF used was 14×10^3 m^2/kg and its specific gravity was 2.2. The Blaine fineness of the GGBS used was 200 m^2/kg and its specific gravity was 2.5.

To reach acceptable workability in silica fume blended concretes and pastes, Sikament NN naphthalene sulphunate-based superplasticizer selected from several available products, was added to mixes. For concrete and pastes mixes water to cementitious material ratios (w/cm) were kept constant to 0.4 and 0.2, respectively. Superplasticizer was well stirred with the total mixing water before adding to the concrete and paste mixes. The specific gravity, water absorption (saturated surface dry) and fineness modulus of the aggregates used in making concrete mixes were 2.6, 3% and 3.72, respectively.

Mixture proportions used in making concretes and pastes are listed in Tables 2 and 3, respectively. Flow table and

Table 2
Characteristics of the concrete mixes made

Concrete mix	Cement/ sand/gravel	W/C	Superplasticizer (%)	Slump approximate (mm)
C-type II	1:1.82:2.39	0.4	1.2	20
C-type II+7% SF	1:1.82:2.39	0.4	1.3	20
C-type II+10% SF	1:1.82:2.39	0.4	1.5	20
C-type II+10% SF+50% GGBS	1:1.82:2.39	0.4	1.5	20

slump test conforming to ASTM C 230 and ASTM C 143 were carried out. All cubic concrete and paste specimens were demoulded after 24 h and 7 days initial curing in tap water was performed. Then, concrete and paste specimens were divided into three groups. First group was moved to simulation ponds which were subjected to artificial immersion and drying cycles alternatively for 180 days, the second group was directly carried to sea coast of Kish Island in the southern Iran, and the third group was kept in tap water tanks until the end of long-term curing (i.e. 180 days). Ionic chemical analyses of pond solution and seawater were the same and have been presented in Table 4 with the chemical analysis of tap water used.

Tap water tank temperature was kept at 20±1 °C. Simulation pond temperature was kept at about 42 and 37 °C according to dominant temperature and time intervals of wetting and drying cycles within tidal zone of south coast of Iran by using electric heater rods for drying and wetting period, respectively. Owing to the fact that wetting and drying cycles were set to occur at 6 hourly intervals and temperature was kept higher than real site environment, the simulation conditions were rather harsher than seacoast environment. The solution in the simulation ponds was refreshed every 2 weeks.

2.2. Test techniques

In this investigation, the deterioration of concrete and pastes were measured by calculating strength change factor (SCF) in percent as follows:

$$SCF = 100\ 3(f_{cw} - f_{cs})/f_{cw}$$

In the above equation, f_{cw} is the average compressive strength of concrete or paste specimens cured in the tap water tank in MPa and f_{cs} is the average compressive strength of concrete and paste specimens cured in the simulation pond or seacoast environment in MPa. The compressive strength tests were carried out on three or four (if necessary) samples cured in tap water tanks, simulation ponds and seawater. In this study, compressive tests were carried out at 3, 7, 28, 90 and 180 days of exposure. After 180 days of exposure to simulation ponds and seawater, samples were evaluated for durability parameters by means of initial water absorption test, chemical analysis, XRD and energy-dispersive X-ray analysis (EDXA). The water absorption tests were carried out on pastes and concrete cubes in accordance with the method specified by RILEM-CPC-11.2 [18] at 180 days of age. Linear correlation between initial water absorption and square root of time was obtained and tangent of the line as pore structure factor (PSF) was projected to evaluate the pore structure of concrete and paste samples. Microstructural studies were conducted on the deteriorated samples to assess the measurements obtained from compressive strength tests. X-ray diffraction (XRD) was performed by the Siemens diffractometer using Cu Kα radiation with wavelength of 1.54 Å and operating at 40 kV and 30 mA. Step scanning was used with a scan speed 2°/min and sampling interval of 0.02°2θ. Samples were examined through scanning electron microscopy and microanalysis (SEM and EDXA) at 180 days curing age, using JOEL 2000EX scanning electron microscope equipped with EDXA analysis system to investigate the microstructure of pastes. Sliced samples cut by diamond wheel saw from the cylinders were epoxy-impregnated, polished and carbon-coated for SEM analysis.

Table 3
Characteristics of the pastes made

Paste mix	W/C	Superplasticizer (%)	Flow (%)
P-type II	0.2	1.5	63±5
P-type II+7% SF	0.2	1.8	64±5
P-type II+10% SF	0.2	2	65±5
P-type II+10% SF+50% GGBS	0.2	2	65±5

Table 4
Concentration of major ions in water used for mixing, initial and control curing together with Kish island seawater and simulation ponds solution

Major constituents	Tap water (ppm)	Seawater/simulation pond (ppm)
Na	173	11,400
K	6	397
Ca	24	450
Mg	16	1600
Cl	372	22,330
SO_4	23	3070

3. Results of the experiments

3.1. Concrete specimens subjected to simulated ponds and seawater tidal zone

3.1.1. Strength change factor

Fig. 1 shows the data obtained on the SCFs of concrete specimens containing silica fume (0%, 7% and 10% of the cement by weight) and silica fume–GGBS (10% SF+50% GGBS) in simulation ponds. The negative SCF values of concrete specimens without silica fume at 28 and 90 days of test signify an increase of compressive strength in simulation ponds condition (f_{cs}), which is most probably attributed to filling up of pores by reaction product and crystallization salt. This phenomenon has also been reported by several investigators [19,20].

Fig. 2 indicates the beneficial effects of partial replacement of silica fume after an immersion period of 28 days in the potable water. This trend continues until the end of test period of 180 days.

The measured compressive strength for SF-10% was the highest, whereas those of mixes with 0% and 7% silica fume

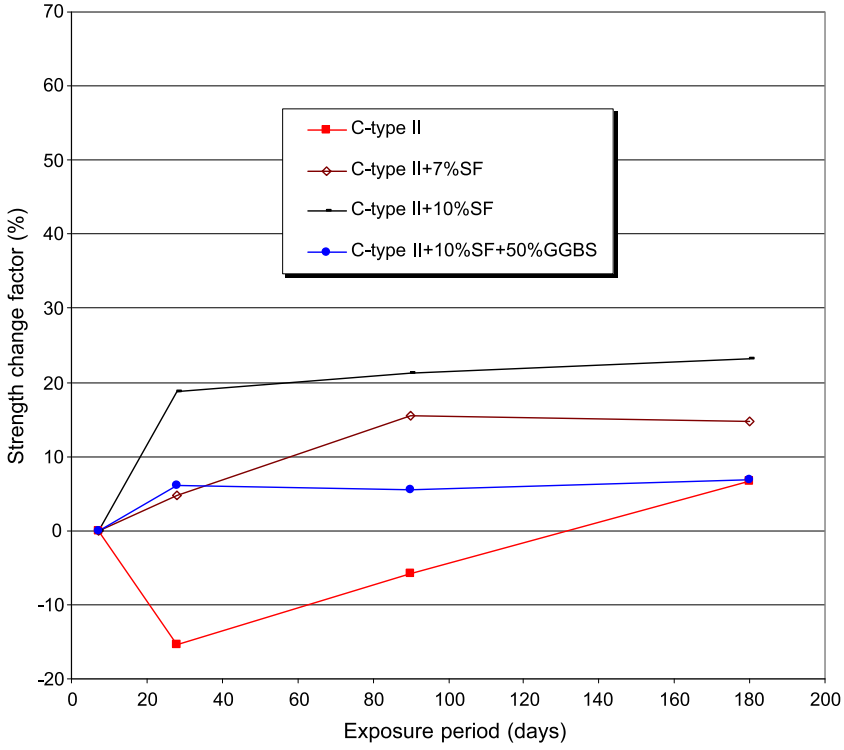

Fig. 1. Variation of strength change factor (SCF) of concrete specimens exposed to simulation ponds.

and SF–GGBS were profoundly lower. This implies that the pozzolanic effect of GGBS was not strong enough to compensate the replaced cement; therefore, the latter specimens showed the lowest strength among all the specimens. However, due to increase in strength of SF specimens, the pozzolanic activity of silica fume used in this investigation is found to be completely acceptable in the potable water.

Nevertheless, with increasing age, as shown in Fig. 1, the strength loss of SF concrete specimens exposed to the simulation pond during test period was more pronounced

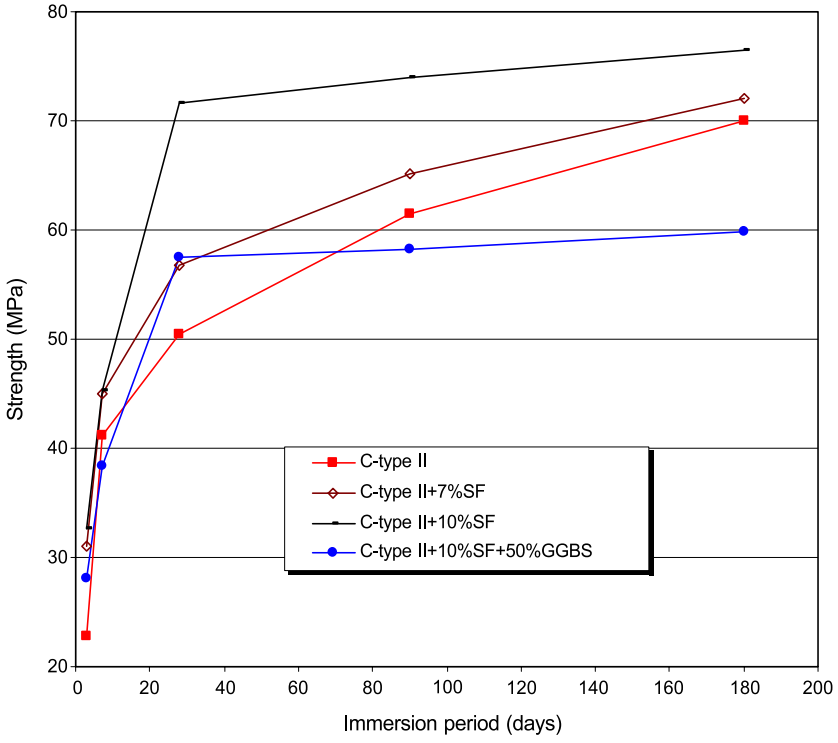

Fig. 2. Compressive strength development with age in concrete specimens immersed in tap water (control curing).

Table 5
Results of absorption by capillary test for concretes (I=absorption percent, x=square root of time)

Concrete mix	Capillary absorption equation	Correlation coefficient	Exposure condition
C-type II	I=0.1762x+0.908	0.97	Tap water
C-type II+7% SF	I=0.1136x+1.1037	0.96	Tap water
C-type II+10% SF	I=0.1303x+0.9177	0.96	Tap water
C-type II+10% SF+50% GGBS	I=0.1507x+0.5141	0.97	Tap water
C-type II	I=0.0399x+0.2396	0.91	Simulation ponds
C-type II+7% SF	I=0.0292x+0.197	0.97	Simulation ponds
C-type II+10% SF	I=.0489x+0.2802	0.99	Simulation ponds
C-type II+10% SF+50% GGBS	I=0.0521x+0.2942	0.98	Simulation ponds

than that of concrete specimens without silica fume. A SCF of 23% was obtained for SF-10% concrete specimens at 180 days curing which was the highest strength change in this group of specimens in the simulation pond. Fig. 1 indicates that the more silica fume added to mixes, the more strength loss obtained.

3.1.2. Initial water absorption

Water absorption measurements were taken at 3, 6, 24 and 72 h and the absorption equations for each mix are given in Table 5 for concrete mixes. The calculated absorption factors are shown in Fig. 3.

3.2. Paste specimens subjected to simulation ponds and seawater tidal zone exposures

3.2.1. Strength change factor

Figs. 4 and 5 show the worse performance of silica fume specimens in simulation ponds and tidal zone exposures. In agreement with the work done by Cohen et al. [14], the increase in the amount of silica fume leads to the higher strength loss and correspondingly the greater SCF. Furthermore, comparing Figs. 4 and 5 shows that replacing 10% of cement with silica fume results in significantly higher SCF than those with 7% silica fume replacement, irrespective of the long-term curing exposure.

Fig. 6 illustrates the beneficial effects of partial replacement of silica fume in control curing condition. Moreover, the compressive strengths of SF-10% paste specimens were higher than that of SF-7%. The optimum percentage of the silica fume replacement used in this research has been reported by Ganjian et al. [21] and was signified by current study as well.

The negative SCF values of some paste specimens in Fig. 4 and all types of pastes in Fig. 5 at 28 days of wetting and drying cycles in sulfates and chloride bearing simulation ponds and tidal zone are attributed to cement hydration developments which are rather fast due to small dimension of specimens. The SCF of paste with 10% silica fume was considerably higher than those pastes with 7% silica fume and without silica fume in simulation ponds exposure. In addition, comparing Figs. 4 and 5 reveals that deterioration in the simulation ponds was stronger than in seawater exposure. Using shorter wetting and drying intervals and constantly higher temperatures in simulation ponds exposure condition, contribute to the above results.

3.2.2. Initial water absorption

Table 6 represents the initial absorption factors for paste specimens. The initial water absorption was correlated linearly to square root of time elapsed. Differences of paste mixes in absorption tangent were plotted in Fig. 7.

3.2.3. X-ray diffraction analysis

The ground and washed with acetone specimens were examined by X-ray machine. The XRD diffractograms of

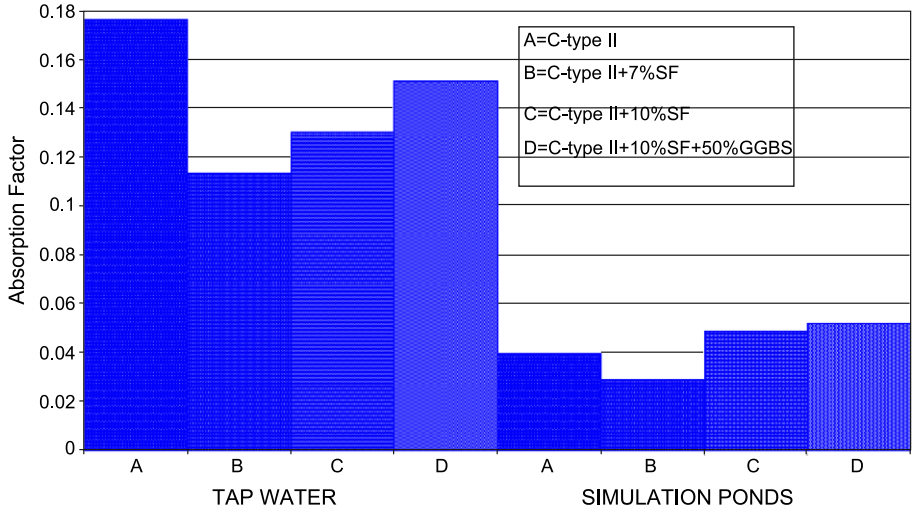

Fig. 3. Absorption coefficient in concretes exposed in different conditions.

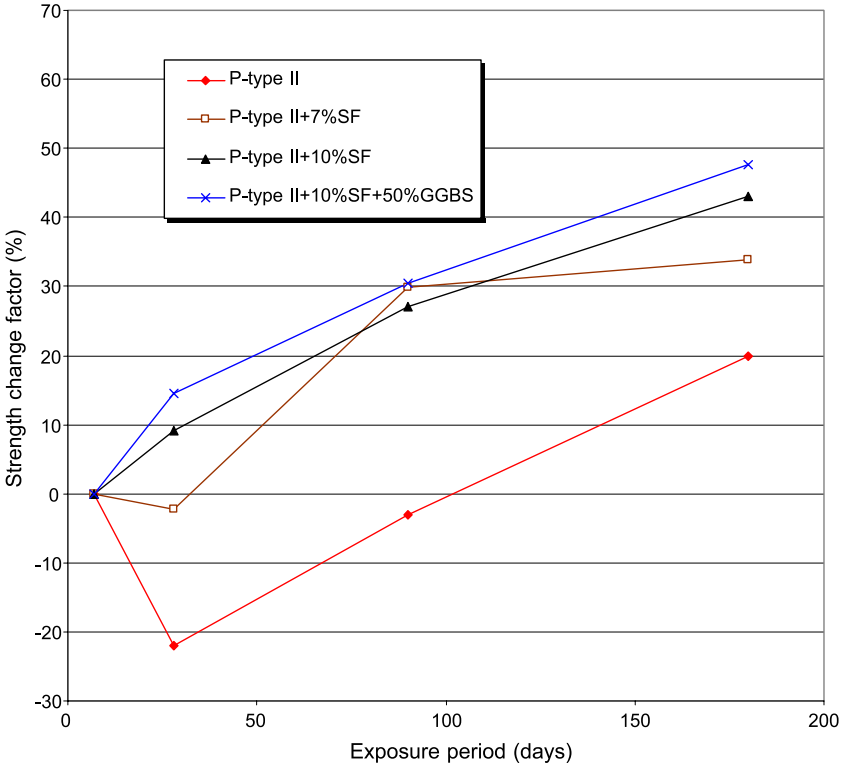

Fig. 4. Variation of strength change factor (SCF) of pastes exposed to simulation ponds.

the powder of paste samples, drawn from two types of mixes and exposure conditions, are presented in Figs. 8–10. The XRD analysis was done on samples at 180 days of exposure to the simulation ponds and the site tidal zone.

Obviously, it can be seen that there were the relatively large intensity peaks for portlandite in no replacement silica fume paste samples cured in site tidal zone (Fig. 8) compared with those with 10% silica fume in simulation ponds and site tidal zone (Figs. 9 and 10). Furthermore, a large quantity of portlandite was converted to gypsum or brucite as seen in Fig. 8. The presence of calcite phase in the examined pastes implies the carbonation effect on surface of specimens which is less in those mixes with silica fume. Ettringite phase was detected in pastes with and/or without silica fume.

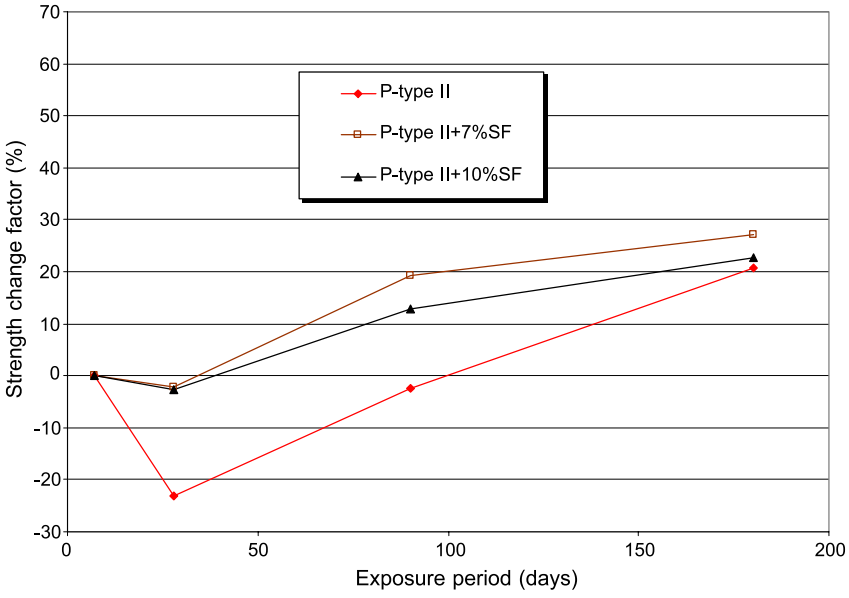

Fig. 5. Variation of strength change factor (SCF) of pastes exposed to site tidal zone.

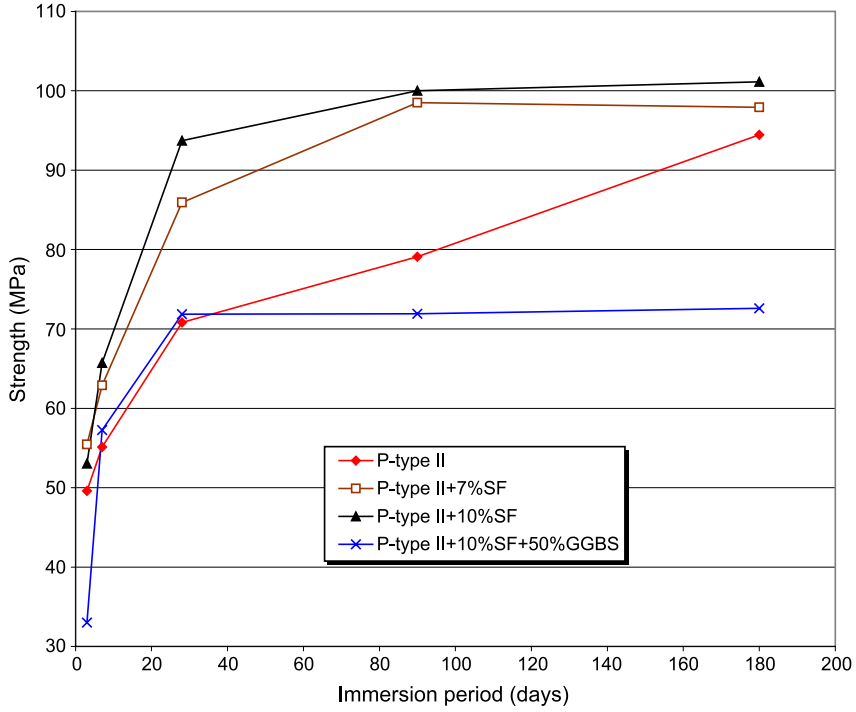

Fig. 6. Compressive strength development with age in paste mixes immersed in tap water (control curing).

3.2.4. Scanning electron microscopy and energy-dispersive X-ray analysis investigations

The microstructures of paste samples exposed to the two long-term exposure conditions at 180 days were observed using SEM. In addition, EDXA analysis was conducted on samples to determine the existing compounds after reactions with external ions. In this procedure, critical areas were point out and energy-dispersive X-ray analysis was conducted. Figs. 11 (area I) and 12 (area II) show EDXA analysis of paste specimen without silica fume cured in the site tidal zone for two different areas at polished surface. A Si peak was easily observed which indicated the presence of C–S–H in the paste; in addition, the formation of ettringite and brucite was confirmed by Fig. 12. Figs. 13 and 14 show EDXA patterns for cement pastes with 10% silica fume replacement in the simulation ponds and site tidal zone at 180 days of exposure. Formation of ettringite together with lower peak of calcium due to pozzolanic reaction was concluded from analysis. These EDXA analyses indicate the absence of brucite in silica fume mixes which is attributed to the lower calcium hydroxide resulting from pozzolanic reaction.

3.2.5. Chemical analysis implications

Chemical analysis was carried out on selected paste specimens to determine bearing compound like magnesium silicate hydrate during the ions in the cementitious matrix at 180 days curing in the tap water and exposure to site tidal zone. The results in Table 7 present the quantitative ions analysis as percent of mass. As expected, the silica fume pastes have more SiO_2 content than those without silica fume. Moreover, higher chloride concentration in the paste specimens exposed to seawater at tidal zone indicates co-existence of sulfates and chloride ions. The high

Table 6
Results of absorption by capillary test for pastes (I=absorption percent, x=square root of time)

Paste mix	Capillary absorption equation	Correlation coefficient	Exposure condition
P-type II	$I=0.3003x+0.881$	0.92	Tap water
P-type II+7% SF	$I=0.1607x+0.492$	0.90	Tap water
P-type II+10% SF	$I=0.131x+0.484$	0.93	Tap water
P-type II+10% SF+50% GGBS	$I=0.1849x+0.0581$	0.98	Tap water
P-type II	$I=0.0701x+0.0824$	0.99	Simulation ponds
P-type II+7% SF	$I=0.1301x+0.1261$	0.99	Simulation ponds
P-type II+10% SF	$I=0.1428x+0.228$	0.99	Simulation ponds
P-type II+10% SF+50% GGBS	$I=0.1945x+0.2133$	0.98	Simulation ponds
P-type II	$I=0.1231x+0.4368$	0.94	Sea water
P-type II+7% SF	$I=0.1275x+0.4791$	0.94	Sea water
P-type II+10% SF	$I=0.1539x+0.4792$	0.96	Sea water
P-type II+10% SF+50% GGBS	$I=0.2077x+0.4982$	0.96	Sea water

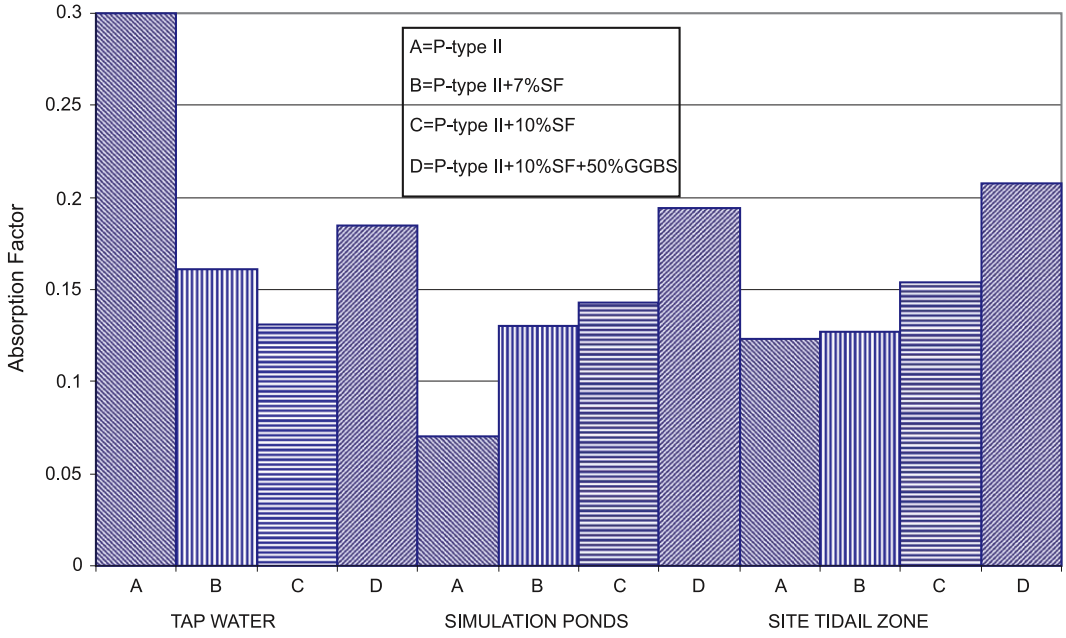

Fig. 7. Absorption coefficient in pastes exposed to different conditions.

magnesium content of different mixes justifies the formation of brucite or any magnesium exposure period in the paste mix P-type II.

4. Discussion

The data provided above indicate that the sulfate attack on silica fume containing concrete and pastes can be different from what is generally proposed. Broadly speaking, replacement of cement ASTM type II, which is known as the best cement to use in both sulfate and chloride bearing environments [21], with silica fume, makes cement pastes more susceptible to sulfate deterioration. Magnesium sulfate is known as the most harmful ingredients in the seacoast of the Persian Gulf [16]. In spite the fact that the concentration of this chemical is not as high as other ions, the lower concentration of the magnesium sulfate can still cause more severe damage to cementitious matrix than other ions in concrete structures [9,22,23].

The silica fume is assumed to be as the reactant to produce secondary C–S–H by consuming calcium hydroxide. The formation of pozzolanic gel begins with hydration of elite and blite during hardening process. Decreased

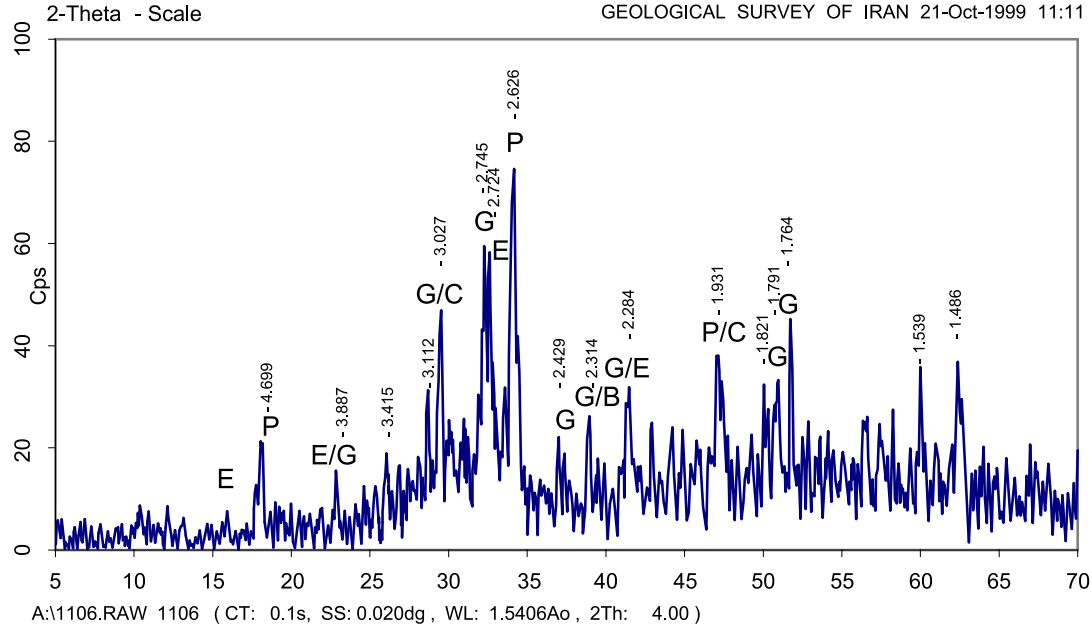

Fig. 8. X-ray diffractogram of the P-type II paste sample exposed to site tidal zone for 180 days. E, ettringite; G, gypsum; P, portlandite; B, brucite; C, calcite.

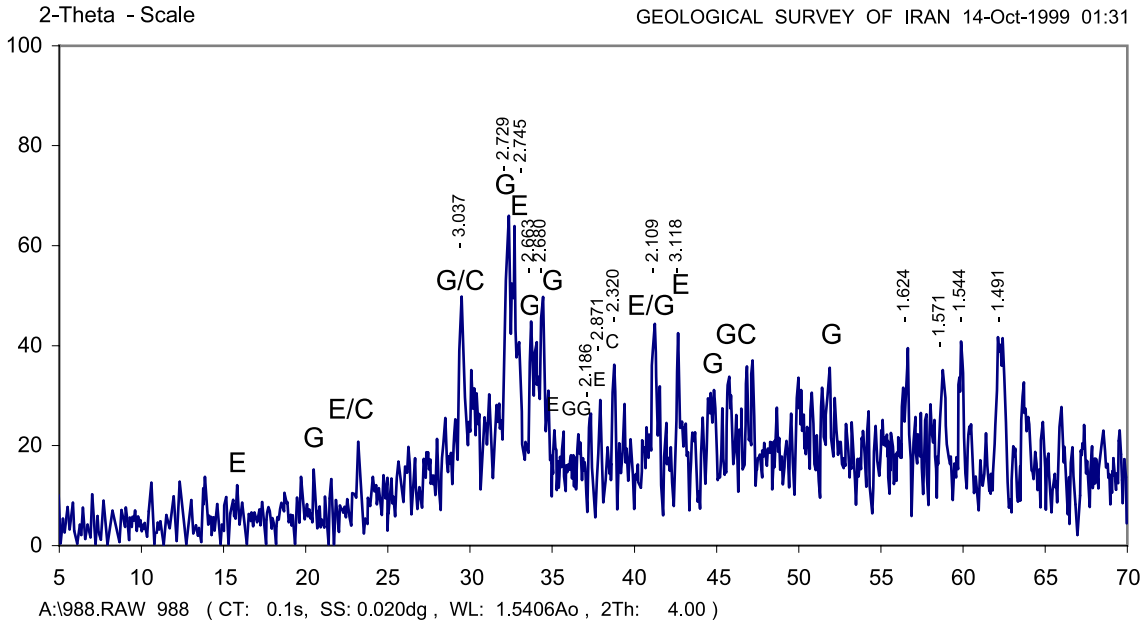

Fig. 9. X-ray diffractogram of the P-type II+10% SF paste sample exposed to simulation ponds for 180 days. E, ettringite; G, gypsum; P, portlandite; B, brucite; C, calcite.

calcium hydroxide content of the cement matrix and increased amount of C–S–H gel together with filler effect of SF contribute to safeguarding of the matrix against external ingressive ions. However, the results from SCF of concrete and paste specimens cured in the simulation ponds and site tidal zone at 180 days of exposure show that the above assumption does not hold; furthermore, the more silica fume replacement leads to more strength loss [6,24]. Contrary to SF specimens, the specimens without silica fume were found to be more resistant to corrosive ions in both the simulation ponds and the site tidal zone. The paste mixes cured in the simulation ponds undergo more deterioration than those exposed to site tidal zone and concrete mixes. These phenomena most probably are attributed to the absence of magnesium hydroxide in silica fume blended pastes and concretes. In particular, the cyclic wetting and drying conditions make it much worse.

Magnesium hydroxide, which is relatively insoluble in water, is known to encompass and block the pores, and protects the C–S–H gel from further attack. Its absence in Portland cement plus silica fume specimens, therefore, makes the C–S–H gel more prone to magnesium sulfate attack. The combined surface double layer of brucite and gypsum protects the hardened cement matrix from magne-

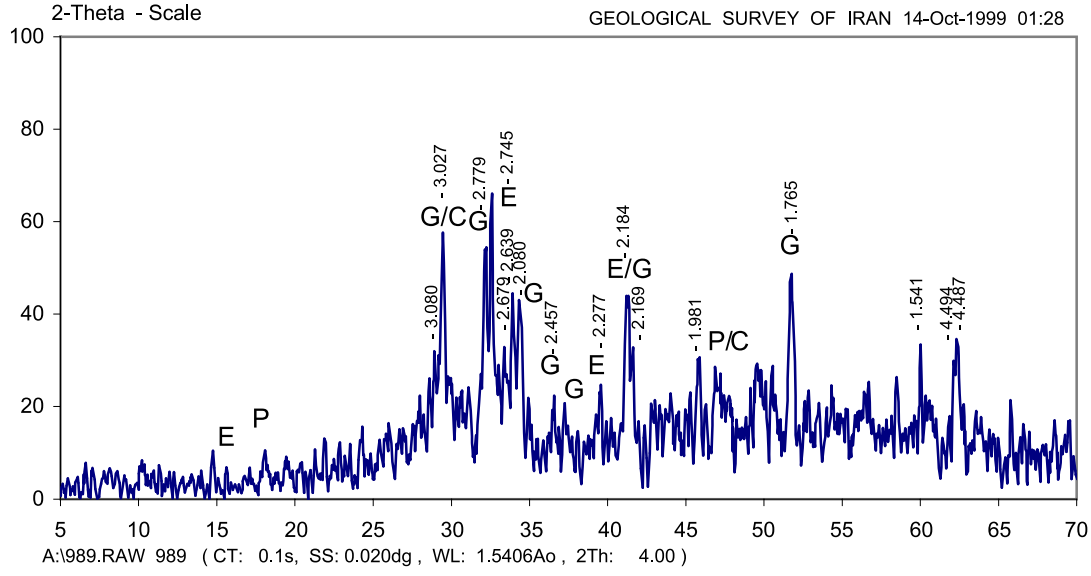

Fig. 10. X-ray diffractogram of the P-type II+10% SF paste sample exposed to site tidal zone for 180 days. E, ettringite; G, gypsum; P, portlandite; B, brucite; C, calcite.

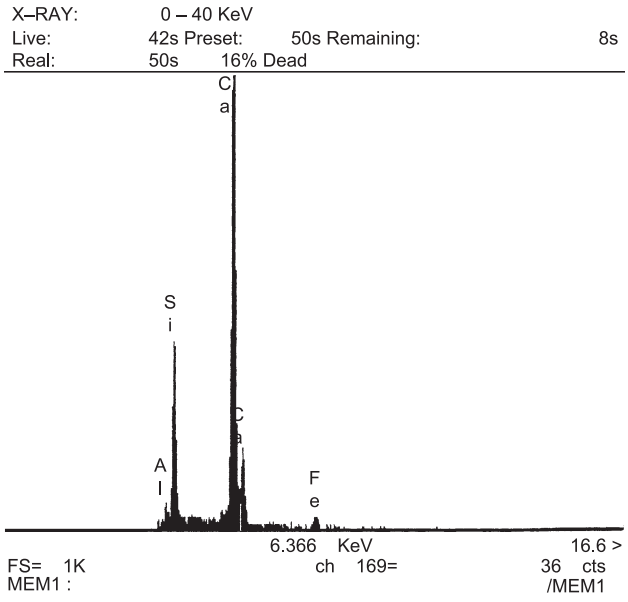

Fig. 11. EDXA profile of the P-type II paste sample exposed to site tidal zone for 180 days. (area I). Si, silicon; Ca, calcium; Al, aluminium; S, sulphur; Mg, magnesium; Fe, ferro.

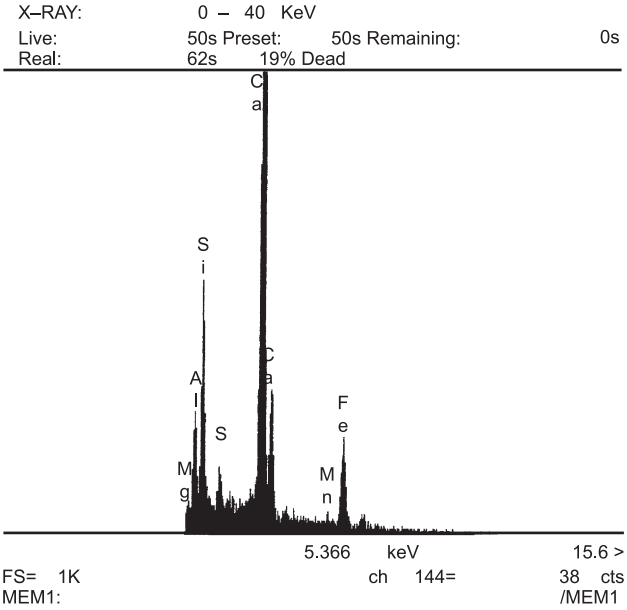

Fig. 12. EDXA profile of the P-type II paste sample exposed to site tidal zone for 180 days. (area II). Si, silicon; Ca, calcium; Al, aluminium; S, sulphur; Mg, magnesium; Fe, ferro.

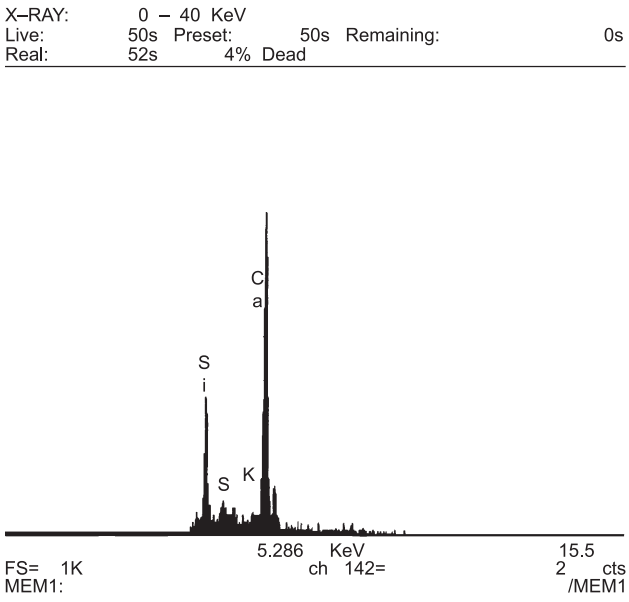

Fig. 13. EDXA profile of the P-type II+10% SF paste sample exposed to simulation ponds for 180 days. Si, silicon; Ca, calcium; Al, aluminium; S, sulphur; Mg, magnesium; Fe, ferro.

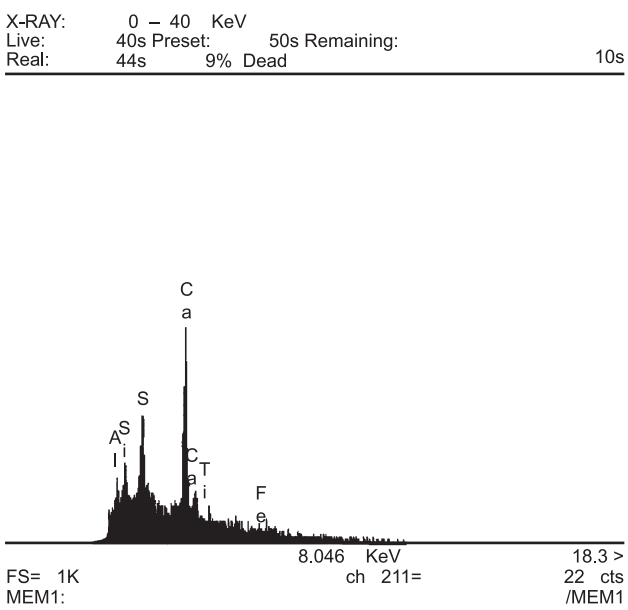

Fig. 14. EDXA profile of the P-type II+10% SF paste sample exposed to site tidal zone for 180 days. Si, silicon; Ca, calcium; Al, aluminium; S, sulphur; Mg, magnesium; Fe, ferro.

sium sulfate attack [12,13]. The greater intensity of the attack may also be the result of the formation of an additional amount of C–S–H gel due to the pozzolanic reaction. This is because the pozzolanic C–S–H gel is different in composition from the C–S–H gel produced by the hydration of alite and belite of Portland cement—'Portland cement C–S–H gel'. This phenomenon was proved by initial water absorption measurement and examination of the microstructure of paste specimens by X-ray diffractometry and EDXA. As shown in Table 6, replacement of cement with silica fume in pastes exposed to simulation ponds and site tidal zone has made tangent of capillary equation to be increased by square root of elapsed time. This increment depends on the amount of silica fume replaced in the mix. The higher the amount of silica fume, the higher the tangent increment (see Figs. 3 and 7). This finding is in accordance with the research results and mechanism developed by Kjellsen [25].

On the other hand, curing in simulation ponds was more aggressive than site tidal zone exposure. This caused more

Table 7
Chemical analysis for cement pastes

Chemical composition (%)	Paste mix/curing condition			
	P-type II	P-type II+10% SF	P-type II	P-type II+10% SF
	Tap water	Tap water	Sea water	Sea water
SiO_2	18.97	22.93	17.97	23.86
Al_2O_3	4.02	3.68	3.95	3.18
Fe_2O_3	2.88	2.84	2.88	2.86
CaO	52.39	50.24	52.86	48.08
MgO	3.41	3.26	3.82	2.90
SO_3	1.62	1.58	2.20	1.97
Na_2O	0.27	0.32	0.31	0.38
K_2O	0.37	0.45	0.36	0.51
Cl	0.014	0.007	0.95	0.70
Loss on ignition	16.4	15.71	15.51	16.06
Free CaO	6.56	2.12	3.8	1.19
Ins. Res.	0.49	0.91	0.35	0.92

strength loss and initial water absorption due to higher and constant temperature of simulation ponds compared to the actual site tidal zone. However, it is noteworthy that in this investigation a considerable reduction in compressive strength of concrete specimens is not observed due to above mechanism. This is because of the size effect and less cement matrix in these concrete specimens. Moreover, longer exposure of these specimens will lead to greater SCFs. In addition, the small accessible pore volume of these concrete specimens due to salt crystallization can be another explanation to the above observation.

In this investigation, the influence of GGBS on durability of concretes and pastes containing silica fume exposed to simulation ponds was also studied. Specimens with dual material replacements have been found to be prone to deterioration against wetting and drying in sulfates. Moreover, the blended optimum GGBS plus SF mix exhibit the lowest strength development in tap water. This can be due to the lower Portland cement contents in these mixes. Furthermore, using GGBS in the mix causes the absorption factor to be profoundly increased in simulation ponds and tidal zone exposure conditions. Therefore it can be concluded that the pore structures of GGBS plus SF mixes under wetting and drying condition in deleterious solutions are more porous than others. The deterioration of binder constitutes of pastes due to magnesium sulfate and decomposition of C–S–H gel to M–S–H, which is uncementitious, can be a probable reason for this phenomenon. The formation of magnesium silicate in different types of cement such as type V cement mortar exposed to magnesium sulfate has been reported by Gollup and Taylor [26]. Also, magnesium silicate formation in concrete exposed to seawater was reported by Cole [27] and by Roy et al. [28] who illustrated that the formation of Mg-rich phases is normally associated with the near surface regions of concrete exposed to Mg-containing solutions, such as seawater. Also, Brown and Doerr [29] established the mechanism by which Mg is transported throughout the pore structures of field concretes with breakthrough of this fact that magnesium hydroxide is known to be highly insoluble in pore solution of concrete. Consequently, the mechanism comprising the effect of mineral admixtures like silica fume and GGBS on M–S–H formation must be taken into account. In addition, the performance of blended cement with silica fume and GGBS has been investigated by several researchers [24,30,31] and reported that different parameters contribute to assessment of durability of these mixes. Further studies are needed to determine the behavior and mechanism of deterioration of dual blended mixes.

5. Conclusions

- Addition of silica fume as the cement replacement, due to pozzolanic reaction, showed enhanced strength development in mixes cured in tap water with direct correlation to amount of cement replacement. The mix with the optimum amount of silica fume exhibited the highest strength development in tap water compared to the blended mixes with optimum GGBS plus silica fume content which exhibited the lowest strength development.
- The performance of pastes and concrete specimens with silica fume exposed to simulation ponds and site tidal zone were inferior to those without silica fume replacement. At 180 days, the best performance was observed for Portland cement type II which exhibited lower strength loss than SF mixes or blended silica fume plus GGBS mixes. The increased rate of SCF was found to be related to silica fume content of concretes and pastes. The more cement replacement with silica fume, the more strength loss achievement.
- From the results of water absorption test, it can be concluded that the capillary absorption factors will be affected considerably by the amount of silica fume. In spite of the fact that SF-10% mixes placed in tap water showed superior performance, those in the simulation ponds revealed higher absorption factor. Furthermore, using GGBS in the mix caused the absorption factor to be profoundly increased in simulation ponds and tidal zone exposure conditions.
- The XRD results showed relatively large intensity peak for the portlandite in the paste specimens with out silica fume; however, ettringite and gypsum were found in all examined pastes. Data gathered through EDXA and chemical analysis confirmed the deterioration mechanism through absence of magnesium hydroxide proposed by other researchers.
- This study indicates that the effect of silica fume in site tidal zone has not been completely understood yet. Different deterioration mechanisms make SF or GGBS cement to be more vulnerable in the magnesium sulfate bearing seawater particularly within tidal zone under

wetting and drying cycles. There is a need for a thorough understanding of influences of the different deterioration mechanisms to assure silica fume potential for improving the durability of concrete structures. With breakthrough of these results, it is recommended that for the long-term durability of concrete in marine and offshore structures, silica fume or GGBS as the cement replacement should be used at low magnesium sulfate concentration waters. To enhance the deterioration resistance of concrete against sulfate and/or salt crystallization, additional protective measures, such as the application of a water-resistant epoxy-based coating, may be considered.

Acknowledgements

The present research described has been carried out in the concrete technology laboratory in department of Civil Engineering, K.N.T. University of Technology, Tehran, Iran. The authors express gratitude to the technicians and the University for the support rendered throughout the research program. The support and site exposure security provided by Kish University of Iran is appreciated.

References

[1] K. Kohno, Relative durability properties and strengths of materials containing finely grounded silica and silica fume, in: Proceeding of the 3rd International Conference on the use of Fly Ash, silica fume, Slag and Natural Pozzolans in Concrete, American Concrete Institute Publication SP-114, Trondheim, Norway, vol. 2, 1989, pp. 815–826.
[2] O. Gautefall, Effect of CSF on the diffusion of chloride through hardened cement paste, in: Proceedings of the 2nd International Conference on the Use of Fly Ash, Silica Fume, Slag and Natural Pozzolans in Concrete, American Concrete Institute Publication SP-91, Madrid, Spain, vol. 2, 1986, pp. 991–998.
[3] M. Maage, T.A. Hammer, Modifisert Portlandsement. Delrapport 3. Fasthetsutvikling og E-modul Report STF65 A85041, FCB/SINTEF, The Norwegian Institute of Technology, Trondheim, Norway, 1985.
[4] H. Cheng-Yi, R.F. Feldman, Hydration reactions in Portland cement–silica fume blends, Cem. Concr. Res. 15 (1985) 585–592.
[5] M.W. Grutzeck, Scott Atkinson, Della M. Roy, Mechanism of Hydration of Condensed Silica Fume in Calcium Hydroxide Solution, Fly Ash, Silica Fume, Slag and Other Mineral By-Products in Concrete, American Concrete Institute Publication SP-79, Detroit, 1983, pp. 643–665.
[6] M.D. Cohen, A. Bentur, Durability of Portland cement–silica fume pastes in magnesium sulfate and sodium sulfate solutions, ACI Mater. J. 85 (3) (1988) 148–157.
[7] M. Maage, Efficiency factors for condensed silica fume in concrete, Third Canmet/ACI Int. Conference on Fly Ash, Silica Fume, Slag and Natural Pozzolans in Concrete, Trndheim, Norway, 1989.
[8] E.J. Sellevold, T. Nilson, Condensed Silica Fume in Concrete: A World Review, Tomas Telford Publications, 1988, pp. 165–246.
[9] W.G. Hime, B. Mather, Sulfate attack or is it, Cem. Concr. Res. 29 (1999) 789–791.
[10] R.S. Gollop, H.F.W. Taylor, Micro structural and micro analytical studies of sulphate attack, Cem. Concr. Res. 22 (1992) 1027–1038.
[11] O.S.B. Al-Amoudi, M. Maslehuddin, M.M. Saadi, Effect of magnesium sulphate and sodium sulphate on the durability performance of plain and blended cement, ACI Mater. J. 92 (1995) 15–24.
[12] F. Turker, F. Akoz, S. Koral, N. Yuzer, Effects of magnesium sulphate concentration on the sulphate resistance of mortars with and without silica fume, Cem. Concr. Res. 27 (1997) 205–214.
[13] D. Bonen, A micro structural study of the effect of produced by magnesium sulfate on plain and silica fume-bearing Portland cement mortars, Cem. Concr. Res. 23 (1993) 541–553.
[14] M.D. Cohen, B. Mather, Sulfate attack on concrete—research need, ACI Mater. J. 88 (1991) 62–69.
[15] T.H. Wee, A.K. Suryavanshi, S.F. Wong, K.M. Anisur Rahman, Sulfate resistance of concrete containing mineral admixture, ACI Mater. J. 97 (2000) 536–549.
[16] P. Ghoddousi, E. Ganjian, T. Parhizkar, A. Ramezanianpour, Conerete Technology, Iran Building and Housing Research Center, Publication No. B 283, Iran, 1998.
[17] E. Ganjian, P. Ghodosi, T. Parhizkar, Mechanical properties of concrete containing Iranian Silica Fume, in: 4th Int. Conf. on Civil Eng., vol. 3, Sharif Univ. of Technology, Tehran, Iran, 1997, pp. 111–123.
[18] RILEM, "CPC-11.2, Absorption of water by concrete by capillarity" TC14-CPC, 1982, RILEM Technical Recommendations for the Testing and Use of Construction Materials, International Union of Testing and Research Laboratories for Materials and Structures, E and FN Spon, England, 1994.
[19] O.S.B. Al-Amoudi, T. Rasheeduzzafar, M. Maslehudin, S.N. Abdul-jauwad, Influence of chloride ions on sulfate deterioration in plain and blended cements, Mag. Concr. Res. 46 (1994) 113–123.
[20] F. Irassar, F. Batic, Effect of low calcium fly ash on sulphate resistance of OPC cement, Cem. Concr. Res. 19 (1989) 194–202.
[21] Z.G. Matta, More deterioration of reinforced concrete in the Arabian Gulf, Concr. Int. (1993 Nov.) 50–51.
[22] A.M. Neville, Properties of Concrete, Fourth Edition, Pearson Education Limited Press, England, 2002.
[23] Y.S. Park, J.K. Suh, J.H. Lee, Y.S. Shin, Strength deterioration of high strength concrete in sulphate environment, Cem. Concr. Res. 29 (1999) 1397–1402.
[24] E.E. Hekal, E. Kishar, E. Mostafa, Magnesium sulfate attack on hardened blended cement pastes under different circumstances, Cem. Concr. Res. 32 (9) (2002) 1421–1427.
[25] K.O. Kjellsen, E.L. Atlassi, Pore structure of cement silica fume systems Presence of hollow-shell pores, Cem. Concr. Res. 29 (1999) 133–142.
[26] R.S. Gollup, H.F.W. Taylor, Microstructural and microanalytical studies of sulfate attack: I. Ordinary Portland cement paste, Cem. Concr. Res. 22 (1992) 1027–1038.
[27] W.F. Cole, A crystalline hydrated magnesium silicate formed in the breakdown of concrete sea-wall, Nature 171 (1953) 354–355.
[28] D.M. Roy, E. Sonnenthal, R. Prave, Hydrotalcite observed in mortars exposed to sulfate solutions, Cem. Concr. Res. 15 (1985) 912–916.
[29] P.W. Brown, A. Doerr, Chemical changes in concrete due to the ingress of aggressive species, Cem. Concr. Res. 30 (2000) 411–418.
[30] J. Frearson, Sulfate resistance of combination of Portland cement and ground granulated blast furnace slag, fly ah, silica fume and natural pozzolans in concrete, Sp-91, ACI, Detroit, MI, 1986, pp. 1495–1524.
[31] M.G. Alexander, B.J. Magee, Durability performance of concrete containing condensed silica fume, Cem. Concr. Res. 29 (1999) 917–922.